

Late reionizations of the Universe and their manifestation in the *WMAP* and future *Planck* data

Pavel Naselsky^{1–3} and Lung-Yih Chiang¹

¹ *Theoretical Astrophysics Center, Juliane Maries Vej 30, DK-2100, Copenhagen, Denmark*

² *Rostov State University, Zorge 5, 344090 Rostov-Don, Russia*

³ *Niels Bohr Institute, Blegdamsvej 17, DK-2100 Copenhagen, Denmark*

Accepted 2003 ???? ???; Received 2003 ???? ???

ABSTRACT

We investigate two sets of two-epoch reionization models and their manifestation in the CMB anisotropy and polarization data of the recent *WMAP* project and make some predictions for the future *Planck* missions. In the first set of models, the universe was reionized twice, first at $z \simeq 15$ by population III stars and then at $z \simeq 6$ by stars in large galaxies. In the second set of models, the extra peak-like reionization at high redshifts $z > 100$ is induced by the decay of unstable particles, followed by the standard picture of reionization at $z \simeq 6$. We examine the general properties of these two-epoch reionization models and their implication in the *WMAP* CMB temperature anisotropy-polarization cross-correlation. We have shown that these models have comparable likelihood values for the *WMAP* data and distinct characters which can be tested with the *Planck* high sensitivities.

Key words: cosmology: cosmic microwave background – physical data and processes: polarization – physical data and processes: atomic processes

1 INTRODUCTION

A detailed study of the ionization history of the Universe is fundamentally important for our understanding of the properties of the structure and evolution of the Universe, particularly the large-scale structure and galaxy formation. Although the epoch of galaxy formation is often referred as the *dark age* due to the difficulty in direct observations, it is, nevertheless, feasible to investigate in details the ionization history of the Universe through the cosmic microwave background (CMB) anisotropies and polarization. The recent CMB experiments, such as the *BOOMERANG* (de Bernardis et al. 2000), *MAXIMA-1* (Hanany et al. 2000), *CBI* (Mason et al. 2002), *VSA* (Watson et al. 2002), *DASI* (Halverson et al. 2002), and its polarization data (Kovac et al. 2002; Leitch et al. 2002) have shed light on probing the dark age of the Universe. In particular, the newly released *WMAP* temperature-polarization data (Hinshaw et al. 2003; Kogut et al. 2003) provide a new way for understanding of the very early stages of galaxy and star formation. We expect to have the future *Planck* polarization data with unprecedented accuracy. The polarization power spectrum from these two missions will therefore provide us the information about the kinetics of hydrogen recombination and allow us to determine the parameters of the last

scattering surface and the ionization history of the cosmic plasma at very high redshifts $z \sim 10^3$.

In the framework of the modern theory of the primary CMB anisotropy and polarization formation, the theory of hydrogen recombination are assumed to be a ‘standard’ one. The classical theory of hydrogen recombination for the pure baryonic cosmological model was developed by Peebles (1968), Zel’dovich, Kurt and Sunyaev (1968), and was generalized for non-baryonic dark matter by Zlotnikov and Naselsky (1985), Jones and Wyse (1985), Seager, Sasselov and Scott (2000), Peebles, Seager and Hu (2000). This standard model of recombination has been modified in various ways.

First of all, there are some variants from the standard hydrogen recombination model, namely, the delay and acceleration of recombination at the redshift $z_{\text{rec}} \simeq 10^3$ due to energy injection from unstable massive particles (Doroshkevich and Naselsky 2002) or due to the lumpy structure of the baryonic fraction of the matter at small scales (Naselsky and Novikov 2002), in which the typical mass of the clouds is of the order $10^5 - 10^6 M_{\odot}$ (see Doroshkevich et al. 2003 and the references therein). Secondly, the most crucial part of the ionization history of the Universe is related to the large-scale structure and galaxy formation and is called late reionization. The model of the late reionization is not yet well-established and needs further investigations.

The conventional view of the ionization history^{*} is that cosmological hydrogen became neutral after recombination at $z_{\text{rec}} \simeq 10^3$ and was reionized at some redshift z_{reion} ,

$$z_{\text{reion}} = 13.6 \left(\frac{\tau_r}{0.1} \right)^{2/3} \left(\frac{1 - \langle Y_p \rangle}{0.76} \right)^{-2/3} \times \left(\frac{\langle \Omega_b h^2 \rangle}{0.022} \right)^{-2/3} \left(\frac{\Omega_{\text{dm}} h^2}{0.125} \right)^{1/3}, \quad (1)$$

where τ_r is the Thomson optical depth, Ω_b is the present baryonic density scaled to the critical density, Ω_{dm} is the dark matter density, $h = H_0/100 \text{ km s}^{-1} \text{ Mpc}$ is the Hubble constant, $\langle Y_p \rangle$ is the helium mass fraction of matter. Recently Cen (2002) has proposed the model of the late reionization with two epochs. Firstly, hydrogen was reionized at redshift $z_{\text{reion}}^{(1)} \simeq 15$ by Population III stars and secondly at $z_{\text{reion}}^{(2)} \simeq 6$ by stars in large galaxies. On the other hand, we also discuss another distinct feature of reionization model, which is called *the peak-like reionization*. This shoot-up in the ionization fraction at $z > 100$ can be induced by energy injection into the cosmic plasma.

These two-epoch reionization models, which can be tested by the *WMAP* and future *Planck* data (Cen 2002), would be significant for the interpretation of the polarization measurements. The polarization of the CMB from the late reionization epoch (or epochs) is sensitive to the width of the period Δz_{reion} , when the ionization fraction x_e increases from the residual ionization ($x_e \sim 10^{-3}$) up to $x_e \sim 0.1 - 1$ (Seljak and Zaldarriaga 1996). They can provide unique information about the physical processes induced by complicated ionization regimes. The aim of the paper is to discuss the distinct characters of these models in the light of recent *WMAP* data and to predict the peculiarities in the polarization power spectrum induced from both the Cen model (2002) of the late reionization and the extra peak-like reionization, taking into account the properties and the sensitivities of the upcoming polarization measurements.

2 PHENOMENOLOGY OF THE TWO-EPOCHED LATE REIONIZATION

The model of the reionization process proposed by Cen (2002) can be described phenomenologically in terms of the injection of additional Ly- c photons via the approach by Peebles, Seager and Hu (2000), Doroshkevich and Naselsky (2002), Doroshkevich et al.(2003). For the epochs of reionization the rate of ionized photon production n_i is defined as

$$\frac{dn_i}{dt} = \varepsilon_i(z) n_b(z) H(z), \quad (2)$$

where $H(z)$ and $n_b(z)$ are the Hubble parameter and the mean baryonic density at z , respectively, $\varepsilon_i(z)$ is the effectiveness of the Ly- c photon production. As one can see from Eq.(??) the dependence of $\varepsilon_i(z)$ parameter upon redshift z allows us to model any kind of ionization regimes, including

^{*} In this paper we refer to ‘‘reionization epoch(s)’’ as epoch(s) with x_e above the residual fraction ($\sim 10^{-3}$) of ionization from the recombination epoch.

heavy particle decays. This parameter also includes uncertainties from the fraction of baryons that collapse and form stars, and the escape fraction for ionizing photons. For late reionization, the ionization fraction of matter $x_e = n_e/n$ can be obtained from the balance between the recombination and the ionization process

$$\frac{dx_e}{dt} = -\alpha_{\text{rec}}(T) n_b x_e^2 + \varepsilon_i(z) (1 - x_e) H(z), \quad (3)$$

where $\alpha_{\text{rec}}(T) \simeq 4 \times 10^{-13} (T/10^4 \text{ K})^{-0.6} \text{ s}^{-1} \text{ cm}^{-3}$ is the recombination coefficient and T is the temperature of the plasma and n_b is the mean value of the baryonic number density of matter. In an equilibrium between the recombination and the ionization process the ionization fraction of the matter follows the well-known regime

$$\frac{x_e^2(z)}{1 - x_e(z)} = \frac{\varepsilon_i(z) H(z)}{\alpha_{\text{rec}}(z) n_b(z)}, \quad (4)$$

where $H(z) = H_0 \sqrt{\Omega_m (1+z)^3 + 1 - \Omega_m}$ and $n_b \simeq 2 \times 10^{-7} (\Omega_b h^2 / 0.02) (1+z)^3$. We would like to point out that Eq.(4) can be used for any models of the late reionization, including the Cen model (2002) by choosing the corresponding dependence of the $\varepsilon_i(z)$ parameter on redshift. This point is vital in our modification of the RECFAST and the CMBFAST packages, from which we can use the standard relation for matter temperature $T(z) \simeq 270 (1+z/100)^2 \text{ K}$ and all the temperature peculiarities of the reionization and clumping would be related with the $\varepsilon_i(z)$ parameter through the mimic of ionization history. For example, in the Cen model (2002) the function $T(t)$ has a point of maxima $T_{\text{max}} \sim (1.3 - 1.5) \times 10^4$ at $z \sim z_{\text{reion}}^{(1)}$ and decreases slowly at $z < z_{\text{reion}}^{(1)}$ down to $T(t) \sim 10^4 \simeq \text{const}$ at the redshift range $6 < z < 12$. Let us introduce some model of the $\varepsilon_i(z)$ parameter dependence over z as

$$\varepsilon_i(z) = \varepsilon_0 \exp \left[-\frac{(z - z_{\text{reion}}^{(1)})^2}{\Delta z_1^2} \right] + \varepsilon_1 (1+z)^{-m} \Theta(z_{\text{reion}}^{(1)} - z), \quad (5)$$

where ε_0 , ε_1 and m are the free parameters, $\Delta z_1 \ll z_{\text{reion}}^{(1)}$ is the width of the first epoch of reionization and $\Theta(x)$ is the step function. The first term of Eq.(5) corresponds to peak-like reionization at $z = z_{\text{reion}}$, which decreases significantly at $z > z_{\text{reion}}^{(1)}$. The second term is related to modelling the second epoch of the reionization model discussed by Cen (2002), which results in a monotonic increasing in $\varepsilon_i(z)$ function as a function of time. From Eq.(5) at $z \simeq z_{\text{reion}}^{(1)}$ we obtain

$$x_e \simeq 1 - \left(\frac{\varepsilon_0 H(z_{\text{reion}}^{(1)})}{\alpha_{\text{rec}}(z_{\text{reion}}^{(1)}) n_b(z_{\text{reion}}^{(1)})} \right)^{-1}, \quad (6)$$

where

$$\begin{aligned} \varepsilon_0 &\gg H^{-1}(z_{\text{reion}}^{(1)}) \alpha_{\text{rec}}(z_{\text{reion}}^{(1)}) n_b(z_{\text{reion}}^{(1)}); \\ &\simeq 10^3 \left(\frac{\Omega_m h^2}{0.125} \right)^{-1/2} \left(\frac{\Omega_b h^2}{0.022} \right) \left(\frac{1 + z_{\text{reion}}^{(1)}}{16} \right)^{0.3}. \end{aligned} \quad (7)$$

One can find from Eq.(4) and (6) that for the second epoch of reionization ($x_e \simeq 1$ at $z \simeq z_{\text{reion}}^{(2)} \simeq 6$ in the Cen model (2002)) the amplitude of the ε_1 parameter and the index m should satisfy the following

$$\varepsilon_1 (1 + z_{\text{reion}}^{(2)})^{-m} \sim \gamma \varepsilon_0, \quad (8)$$

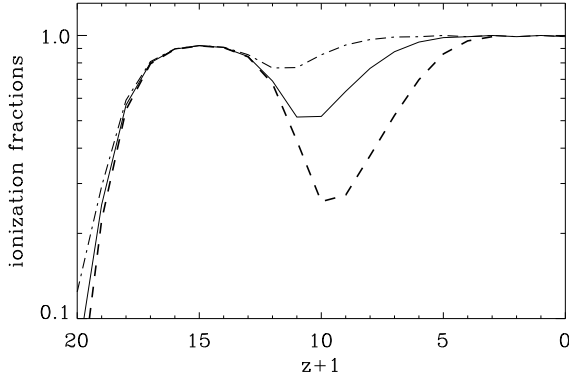


Figure 1. The ionization fraction for the two-epoch reionization models. Solid line corresponds to the model 1, the dash line the model 2 and the dash-dot line the model 3.

where γ is the parameter between 0.1 to 1 in order to model the properties of the Cen model and its variants. We demonstrate the effectiveness of our phenomenological approach in Fig. 1: the ionization fraction x_e against redshift for the three models listed below:

- model 1: $\varepsilon_0 = 1.3 \times 10^3, \varepsilon_1 = \beta \times 10^9, \beta = 1, m = 7$;
- model 2: $\varepsilon_0 = 1.3 \times 10^3, \varepsilon_1 = \beta \times 10^9, \beta = 0.1, m = 7$;
- model 3: $\varepsilon_0 = 1.3 \times 10^3, \varepsilon_1 = \beta \times 10^9, \beta = 100, m = 8$.

The curves are produced from the modification of the RECFAST code (Seager, Sasselov and Scott 2000). Obviously the model 2 (dash line) is not physically viable, we nevertheless can use it to test the sensitivity of CMB polarization to non-monotonic shape of ionization fraction. For all models we use the following values of the cosmological parameters: $\Omega_b h^2 = 0.022, \Omega_m h^2 = 0.125, \Omega_\lambda = 0.7, h = 0.7, \Omega_m + \Omega_\lambda = 1$. We show the 3 models in Figure 1. Model 1 and 2 mimic the properties of the Cen model (2002) where there is a dip in the reionization fraction, whereas model 3 corresponds to roughly the standard reionization model with no significant presence of peaks in ionization fraction.

3 THE CMB POLARIZATION FOR THE TWO-EPOCHED LATE REIONIZATION MODELS

In order to find out how sensitive the polarization power spectrum is to the two-epoch reionization models, we consider phenomenologically the different variants of hydrogen reionization models by modifying the RECFAST (Seager, Sasselov and Scott 2000) and CMBFAST code (Seljak and Zaldarriaga 1996). In Fig. 3 we plot the polarization power spectrum $C_p(\ell)$ for the model 1, 2, the standard single reionization model at $z_{\text{reion}} \simeq 6$ and 13.6. The difference between model 1 and 2 mainly lies in between the multipoles $2 < \ell < 30$.

3.1 The anisotropy and polarization in comparison with the WMAP data

To characterize the differences between the reionization models we have used the WMAP programme (Verde et

Filter	Cen model		
model variants	1	2	3
Likelihood (T)	-494.357	-525.928	-495.159
Likelihood (TE)	-231.601	-223.749	-230.766

Table 1. The likelihood parameters of the variants of the Cen model (2003).

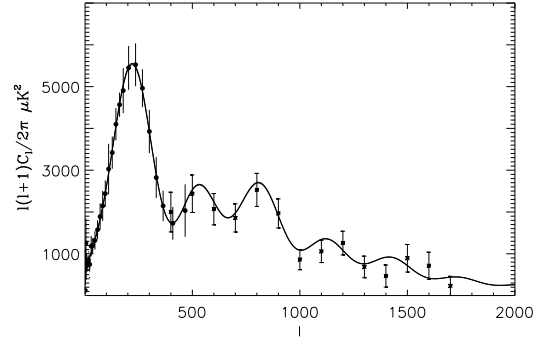


Figure 2. The anisotropy power spectrum for models 1 – 3 in comparison with WMAP and CBI data. All the models predict approximately the same shape which cannot be seen in the figure due to degeneracy. The corresponding likelihood parameters are shown in Table 1. The WMAP data are taken from the official website at the range $\ell \leq 500$. The CBI data are taken from CBIM1 and M2 data sets.

al. 2003) for the calculations of the likelihood for the anisotropy and TE correlation power spectra against those from WMAP results, shown in Table 1. As one can see, for all the models of late reionization we get fairly good consistency for anisotropy and the TE correlations. The accuracy of the WMAP data (Hinshaw et al. 2003; Kogut et al. 2003) however is not enough for discrimination between the models. Therefore, the future Planck data is required for more accurate investigations of the history of hydrogen reionization at relatively low redshifts $z < 30$. For comparison, the WMAP best-fitting cosmological model has the likelihood parameter -486.245 (with 900 data points) for the anisotropy and -228.695 (with 499 data points) for the TE cross-correlation. As one can see from Table 1, all the models have excellent agreement with the WMAP data, but we are not able to distinguish with the accuracy of the WMAP data between the two-epoch reionization models in the Cen model (2002). In order to check the high multipole range of the power spectrum of temperature anisotropies in the models 1 – 3, in Fig. 2 we plot the $C(\ell)$, which are almost indistinguishable for all the models and are consistent with the WMAP and the CBI data. The result shows excellent agreements between the theoretical curves and the data points from the experiments. The most intriguing question is could the future Planck data sets allow us to distinguish any peculiarities of the late reionization epochs?

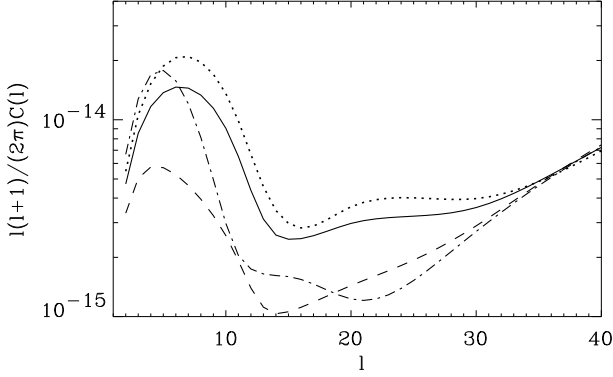


Figure 3. The polarization power spectrum for different models of the reionized universe. The solid line corresponds to the model 1, the dotted line the model 2, the dash and the dash-dot line are the model with single reionization ($x_e(z_{\text{reion}}) = 1$) at $z_{\text{reion}} \simeq 6$, and at $z_{\text{reion}} \simeq 13.6$, respectively.

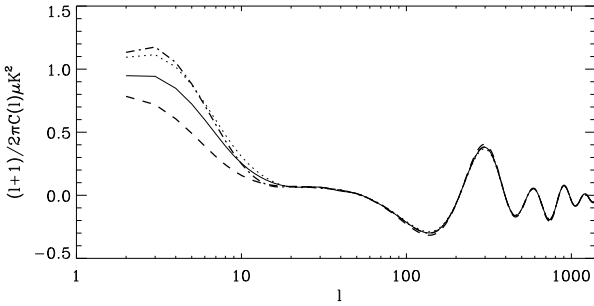


Figure 4. The TE cross-correlation power spectrum for different models of the reionized universe. The solid line corresponds to the model 1, the dotted line the model 2, the dash and the dash-dot line are the model with single reionization ($x_e(z_{\text{reion}}) = 1$) at $z_{\text{reion}} \simeq 6$, and at $z_{\text{reion}} \simeq 13.6$, respectively.

3.2 The anisotropy and polarization in comparison with the future *Planck* sensitivity

The differences between the late reionization models in comparison with the expected sensitivity of the *Planck* mission can be expressed in terms of the power spectrum $C_p(\ell)$ (for the anisotropy, E and TE component of polarization)

$$D_{i,j}(\ell) = \frac{2[C_{p,i}(\ell) - C_{p,j}(\ell)]}{C_{p,i}(\ell) + C_{p,j}(\ell)}, \quad (9)$$

where the indices i and j denote the different models.

In order to clarify the manifestations of the complex ionization regimes in the models 1 and 2 we need to compare the peak to peak amplitudes of the $D_{i,j}(\ell)$ function with the expected error of the anisotropy power spectrum for the *Planck* experiment. We assume that the systematics and foreground effects are successfully removed. The corresponding error bar should be

$$\frac{\Delta C(\ell)}{C(\ell)} \simeq \frac{1}{\sqrt{f_{\text{sky}}(\ell + \frac{1}{2})}} [1 + w^{-1} C^{-1}(\ell) W_\ell^{-2}], \quad (10)$$

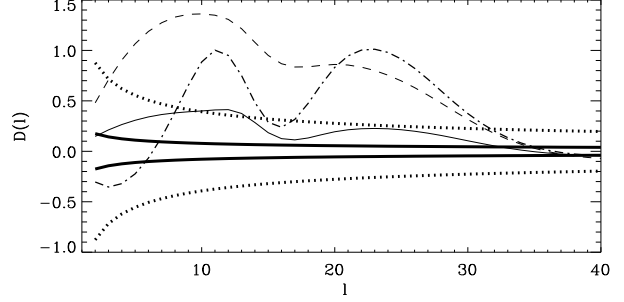


Figure 5. The plot of $D_{i,j}$, the deviation in polarization for different reionization models. The solid line $D_{2,1}$ corresponds to the models 1 and 2, the dash-dot line $D_{s,1}$ is from the model 1 in comparison with the model of single reionization at $z_{\text{reion}} \simeq 13.6$ and the dash line $D_{s,1}$ is from the model 1 in comparison with the model of single reionization at $z_{\text{reion}} \simeq 6$. The thick solid (binning) and dotted curves ($f_{\text{sky}} = 0.65$, no binning) mark the estimated *Planck* errors.

where $w = (\sigma_p \theta_{\text{FWHM}})^{-2}$, $W_\ell \simeq \exp[-\ell(\ell+1)/2\ell_s^2]$, $f_{\text{sky}} \simeq 0.65$ is the sky coverage during the first year of observations, σ_p is the sensitivity per resolution element $\theta_{\text{FWHM}} \times \theta_{\text{FWHM}}$ and $\ell_s = \sqrt{8 \ln 2} \theta_{\text{FWHM}}^{-1}$.

For all *Planck* frequency channels, for example, the FWHM are less than 30 arcmin, so for the estimation of the errors at $\ell \leq 40$ range we can omit the second term in Eq. (10). In Fig.3 we show the polarization power spectrum and TE cross-correlation for models. While polarization power spectrum is not observed by WMAP, the upcoming *Planck* mission will be able to provide us the observation to differentiate different models. It is clear from Fig.4 that the TE cross-correlation spectra for different regimes of reionization have different shape at $\ell \leq 10$ range but do not vary significantly for $\ell > 10$. All the deviations lie inside the cosmic variance and are practically not observable.

As one can see from Fig. 5 for $D_{1,2}(\ell)$ the corresponding peak to peak amplitudes are on the order of magnitude 20% at $\ell \sim 10 - 40$, while the errors $\Delta C(\ell)/C(\ell)$ are in about the same one. Such small deviations in the polarization power spectrum caused by the complicated ionization regimes can not be tested directly for each multipole of the $C(\ell)$ power spectrum by the *Planck* mission, even the systematic effects would be removed down to the cosmic variance level.

As shown in Fig. 5, the deviation $D_{2,1}$ mostly lies inside the error region. This indicates that the upcoming *Planck* observational data would not be able to distinguish the two-epoch late reionization models from each other, where the only difference is in the amplitudes of the minima of ionization fraction. However, it is worth noting that both the models 1 and 2 have significant deviation from the standard single reionization model (the dash and the dash-dot line).

The shape of the polarization power spectrum in the two-epoch late reionization model differs from the shapes for single reionization models even for $z_{\text{reion}} \simeq 13.6$. Such kind of dependence is related to the difference with Δz of the epoch when the ionization fraction starts to grow from $x_{e,\text{min}} \sim 10^{-3}$ up to $x_{e,\text{max}} \sim 1$.

An unique possibility to detect more complicated structure of late reionization would be from the binning of the initial data, using, for example, the same range of bin $\sim 15 - 30$.

In such case, if the correlations between each multipole are small, the accuracy of the $C(\ell)$ estimation would be approximately 4–5 higher than for unbinned power spectrum and non-monotonic structure of the $D(\ell)$ function could be detectable for the anisotropy and for E and TE polarization as well.

4 PEAK-LIKE REIONIZATION AT HIGH REDSHIFTS

In this section we shall investigate another type of two-epoch reionization models. What is the implication of another reionization occurring at high redshifts, if, for example, one of the epochs of the pre-reionization took place at redshifts $30 \ll z < 1000$? Note that for $z \gg 30$ the Compton cooling of the plasma is extremely important and any energy injection to the cosmic plasma could produce relatively short epochs of reionization, when the ionization fraction became significantly higher ($x_{e,\max} \sim 1$), but for relatively short time interval. We call such distinct character of reionization *the peak-like reionization*. Such regimes can be induced by the decay or annihilation of some unknown particles or decay of the primordial black holes (Naselsky 1978; Ivanov, Naselsky and Novikov 1994; Kotok and Naselsky 1998) during the long period $3 \times 10^5 - 10^8$ years. Because of the Compton cooling of the plasma the injected energy density ϵ_{inj} would be absorbed by the CMB photons leading to y -distortion in the black-body spectra. Peebles, Seager and Hu (2000) have shown that the corresponding value of the y -parameter in this model is $y \sim 0.25\epsilon_{\text{inj}}/\epsilon_{\text{CMB}}$, where ϵ_{CMB} is the energy density of the CMB at the redshift of the injection. Taking into account the *COBE* upper limit for y -parameter (Fixen et al. 1996) $y_{\text{cobe}} < 2 \times 10^{-5}$, one can estimate the upper limit of the energy injection $\epsilon_{\text{inj}} < 4y_{\text{cobe}}\epsilon_{\text{CMB}}$. On the other hand, for reionization of each hydrogen atom we need to have roughly one photon with energy $E \simeq I$, where $I \simeq 13.6\text{eV}$. Thus, $\epsilon_{\text{inj}} \sim x_e I n_b$ and we obtain the limit

$$x_e \leq 4y_{\text{cobe}} \left(\frac{\epsilon_{\text{CMB}}}{I n_b} \right) = 4y_{\text{cobe}} \left(\frac{m_p}{I} \right) \left(\frac{\epsilon_{\text{CMB}}}{\epsilon_b} \right) \sim 10^2 (1 + z_{\text{inj}}) \left(\frac{\Omega_b h^2}{0.022} \right)^{-1} \quad (11)$$

where $m_p \simeq 1\text{ GeV}$ is the proton mass and ϵ_b is the energy density of baryons at redshift z_{inj} . From Eq.(11) it is clear that the peak-like reionization ($x_e \sim 1$) is self-consistent with the *COBE* observational limit on y -parameters. We can describe the peak-like reionization in terms of the injection of an additional Ly- c photons as in Section 1, but with the source term now the Dirac δ -function

$$\frac{dn_i}{dt} = \eta n_b(z) \delta_D(t - t_p), \quad (12)$$

where η is the effectiveness of the Ly- c photon production, and t_p is the age of the Universe at the moment of peak-like reionization. Thus for the ionization fraction x_e we get

$$\frac{dx_e}{dt} = -\alpha_{\text{rec}}(T) n_b x_e^2 + \eta (1 - x_e) \delta(t - t_p). \quad (13)$$

Quantitatively we can assume that for the first reionization epoch the maximum of the ionization fraction is small ($x_e \ll 1$) and we neglect x_e in the $1 - x_e$ term in Eq.(13). In

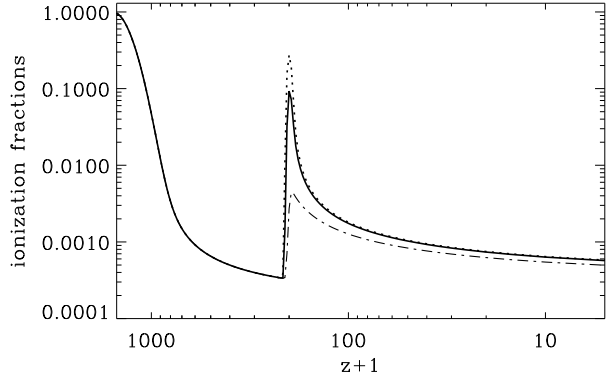


Figure 6. The ionization fraction for the peak-like reionization model (model 4). The dotted, the solid and the dash-dot lines correspond to model 4a, 4b and 4c.

such an approximation the ionization balance of plasma is determined by the pure balance between the recombination term and the energy injection term in Eq.(12):

$$x_e(t) \simeq \eta \left(1 + \eta \int_{t_p}^t \alpha(T) n_b dt \right)^{-1}, \quad (14)$$

for the temperature of the plasma we can assume that $T(t_p) \sim (1 - 2) \times 10^4\text{ K}$ and at $t > t_p$,

$$\frac{dT}{dt} = \frac{T_{\text{CMB}} - T}{\tau_c}, \quad (15)$$

where τ_c is the Compton cooling time. Note that our assumption about maxima of $T(t_p) \sim 10^4\text{ K}$ is closely related with the energy balance. For reionization of the hydrogen by electromagnetic cascades the typical energy release is in the order $I n_b x_e$. Such a part of the energy of a cascade does not behave as a simple δ -function in the energy spectrum (see Doroshkevich & Naselsky 2002) and is usually characterised by power law $E^{-\gamma}$. Because of Compton scattering of high energy γ -quanta off electrons, it is natural to estimate the kinetic energy of electrons as $n_b kT \sim I n_b x_e$ and $T \sim I x_e / k \sim 10^4\text{ K}$ where k is the Boltzmann constant. At $z > 40$ the ratio between characteristic time of recombination $t_{\text{rec}} = [\alpha(T = 10^4\text{ K}) n_b]^{-1}$ and τ_c is more than one order of magnitude, while both of them are much smaller than the Hubble time. The relaxation of the matter temperature to the CMB temperature proceeds faster than the ionized hydrogen becoming neutral. Thus, while the temperature of matter is close to the CMB temperature T_{CMB} , the corresponding time of recombination is

$$\Delta t_{\text{rec}} \simeq \frac{x_e}{|dx_e/dt|} \simeq \eta^{-1} t_r(T_{\text{CMB}}), \quad (16)$$

where $t_r = t_{\text{rec}}$ at $T = T_{\text{CMB}}$. Taking into account the above-mentioned properties of the temperature history of the plasma we can estimate the Thomson optical depth $\Delta\tau_r$ caused by the peak-like reionization as follows

$$\Delta\tau_r \simeq \tau_r \left(\frac{t_r}{t_p} \right) \ln \left(1 + \eta \frac{t_p}{t_r} \right), \quad (17)$$

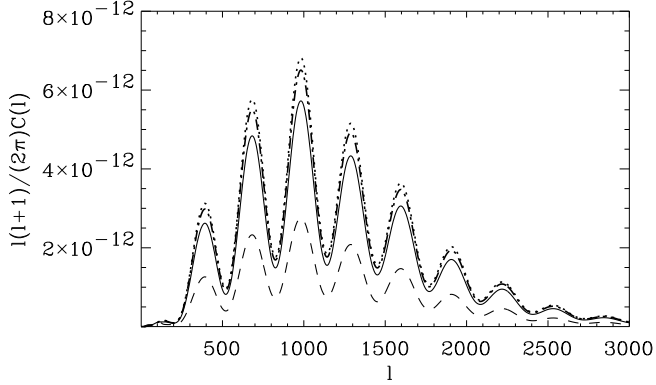


Figure 7. The polarization power spectrum for the extra peak-like reionization models (the model 4). The dash, the solid and the dash-dot line correspond to the model 4a, 4b and 4c, respectively. The dotted line is the standard single reionization model at $z_{\text{reion}} \simeq 6$.

where τ_r satisfies Eq.(1) at $z_{\text{reion}} = z_{\text{reion}}(t_p)$. For example, if the peak-like reionization takes place at the redshift $z_{\text{reion}} = 200$ and $\eta \simeq 0.1 - 0.2$ then

$$\frac{t_r}{t_p} \simeq 0.1(1 + z_{\text{reion}})^{-0.9} \left(\frac{\Omega_b h^2}{0.022} \right) \left(\frac{\Omega_m h^2}{0.125} \right)^{-1/2}, \quad (18)$$

and the corresponding values of the optical depth from Eq.(17) are in order of the magnitude $\Delta\tau_r \simeq 0.03 - 0.05$. As one can see, if the CMB anisotropy data are consistent with the limit on Thomson optical depth of reionization $\tau_r \leq 0.1$ (Doroshkevich, Naselsky, Naselsky and Novikov 2003), then roughly 30–50% of τ_r can be induced by the peak-like reionization and 50–70% with the late reionization caused by the structure formation at low redshifts. To describe the peak-like reionization numerically we use a Gaussian approximation for the energy injection in Eq.(12)

$$\eta\delta(t - t_p) \rightarrow \xi H(z) \exp \left[-\frac{(z - z_{\text{reion}})^2}{(\Delta z)^2} \right] \quad (19)$$

and describe the following two sets of examples for the peak-like reionization:

- model 4a: $z_{\text{reion}} = 200$ with $\Delta z = 5$, $\xi = 100$;
- model 4b: $z_{\text{reion}} = 200$ with $\Delta z = 5$, $\xi = 10$;
- model 4c: $z_{\text{reion}} = 200$ with $\Delta z = 5$, $\xi = 1$,

and

- model 5a: $z_{\text{reion}} = 500$ with $\Delta z = 12.5$, $\xi = 100$;
- model 5b: $z_{\text{reion}} = 500$ with $\Delta z = 12.5$, $\xi = 10$;
- model 5c: $z_{\text{reion}} = 500$ with $\Delta z = 12.5$, $\xi = 1$,

where $\Delta z/z_{\text{reion}} = 0.025$ for both sets of models. The late reionization $x_e(z \simeq 6) = 1$ at $z \simeq 6$ is included in both model 4 and model 5, as it is the standard part of the CMBFAST package. In Fig. 6 we plot the shape of the ionization fraction of the plasma x_e for the model 4. As an analytical description, one can see the peaks of x_e at $z_{\text{reion}} = 200$, which drops down at $z \sim 100 - 150$.

By modification of the CMBFAST code for the primary polarization, we plot in Fig. 7–9 the corresponding power spectrum for the model 4 and 5. As one can see from Fig. 7

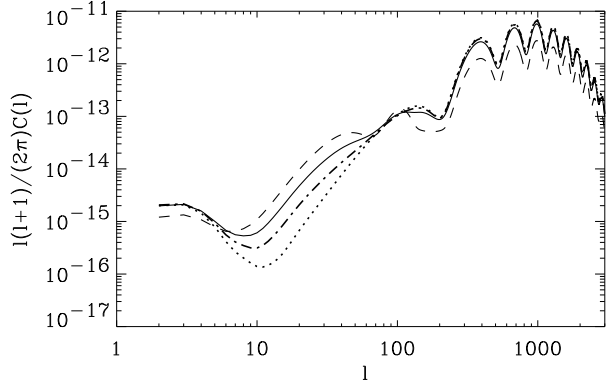


Figure 8. The polarization power spectrum for the model 4 as in Fig. 7 but in logarithmic scale, in which the differences between the power spectra can be seen more clearly at the multipole range $\ell < 100$.

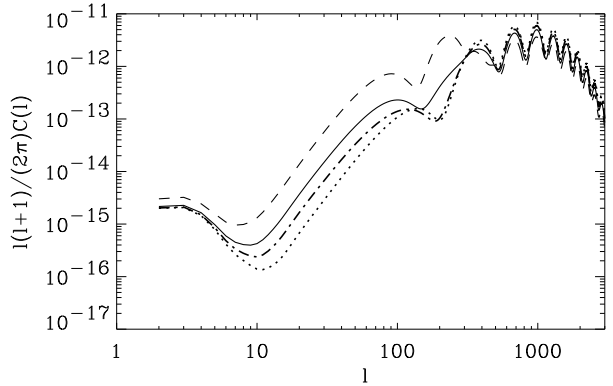


Figure 9. The polarization power spectrum for the extra peak-like reionization models (the model 5) in logarithmic scale. The dash, the solid and the dash-dot line correspond to the model 5a, 5b and 5c, respectively. The dotted line is the standard single reionization model at $z_{\text{reion}} \simeq 6$.

the common manifestation of the extra peak-like and the standard late reionization produce interesting features in the power spectrum. Namely, for high multipoles ℓ the amplitude of the power spectrum decrease as $\exp(-\tau_r)$, while for the multipole range $\ell < 100$ the manifestation of the peak-like reionization is very clear, in particular at $10 < \ell < 200$ from Fig. 8. Figure 9 shows how important the peak-like reionization at $z_{\text{reion}} = 500$ could be for the distortion at higher multipole range of the polarization power spectrum. In Fig. 10 we plot the $D_{4,s}$ function, the comparison between the model 4 and the standard single reionization model at $z_{\text{reion}} \simeq 6$. Fig. 11 is the comparison between the model 5 and the standard single reionization model at $z_{\text{reion}} \simeq 6$. In Table 2, we show the calculated likelihood for the anisotropy and TE correlation power spectra from the model 5 against those from *WMAP* results (Hinshaw et al. 2003; Kogut et al. 2003). They are close to the parameters from the model 4.

Once again we would like to point out that all the peculiarities induced by the extra peak-like reionization have

Filter	peak-like model		
	5a	5b	5c
model variants	5a	5b	5c
Likelihood (T)	ruled out	-770.693	-509.583
Likelihood (TE)	-341.908	-261.204	-236.388

Table 2. The likelihood of the variants of the peak-like model (model 5).

localized structure which appears at some fixed multipole range. These features can be tested by the *Planck* polarization measurements.

5 CONCLUSIONS

We have investigated the two-epoch reionization models of the Universe. The two-epoch reionization can be induced by the structure formation as described in Cen model (2002), or caused by unknown sources of the energy injection (peak-like reionization) at relatively high redshifts $z > 30$. We have shown that for the Cen model (2002) the *WMAP* and the *Planck* mission would be able to detect the general shape of the ionization history for the two-epoch reionized plasma, which differs from the single reionization models at $z \simeq 13.6$ or $z \simeq 6$. However, any peculiarities of the ionization fraction of the matter inside the range $6 < z < 13.6$, such as the decreasing of ionization, do not observed by the *WMAP* experiment due to the statistical significance from the cosmic variance effect. The peak-like reionization model, on the other hand, has some distinct features in the shape of ionization fraction, and of the polarization power spectrum as well. The most pronounced manifestation of the peak-like reionization model is the localized features in the polarization power spectrum which differs from the standard single reionization model. We reckon that such kind of deviation from the standard reionization model, in case of confirmation by the *Planck* data, will be significant for investigation of unstable particles or any relic decaying during the ‘dark age’ of the Universe.

Note that in this paper we do not consider the secondary anisotropies and polarization produced by the peak-like reionization at high redshifts. These effects seem to be important if we take into account the fact that the relaxation of the peculiar velocity of baryonic matter and dark matter at $z \simeq 200$ is completed and we can have the analog of the Ostriker-Vishniak effect and the Doppler effect, but for specific shape of the ionization fraction. These effects will be investigated in the next paper.

ACKNOWLEDGMENTS

This paper is supported in part by Danmarks Grundforskningsfond through its support for the establishment of the Theoretical Astrophysics Center.

REFERENCES

Bennett C. L. et al., 1995, BAAS, 187.7109

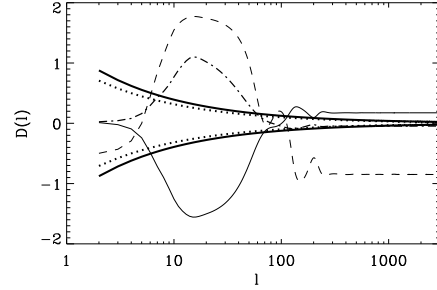


Figure 10. The plot of $D_{4,s}$ for comparison between the model 4 and the standard single reionization model at $z_{\text{reion}} \simeq 6$. The solid line represents $D_{4a,s}$, the model 4a and the standard single reionization model $z_{\text{reion}} \simeq 6$. The dash line $D_{4b,s}$ between the model 4b and the standard at $z_{\text{reion}} \simeq 6$ and the dash-dot line $D_{4c,s}$ between 4c and the standard at $z_{\text{reion}} \simeq 6$. The thick-dotted ($f_{\text{sky}} = 0.65$) and solid lines ($f_{\text{sky}} = 1$) represent the cosmic variance limit for the *Planck* missions.

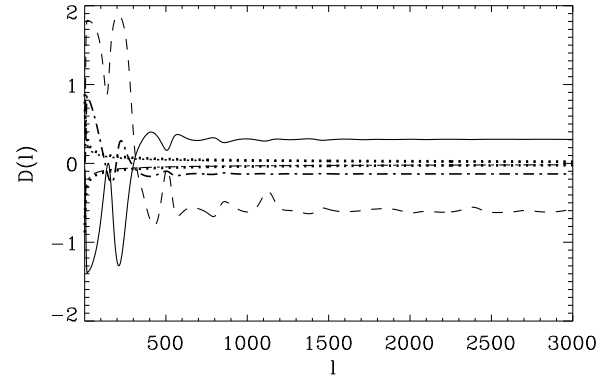


Figure 11. The plot of $D_{5,s}$ for comparison between the model 5 and the standard single reionization model at $z_{\text{reion}} \simeq 6$. The solid line represents $D_{5a,s}$, the model 5a and the standard single reionization model $z_{\text{reion}} \simeq 6$. The dash line $D_{5b,s}$ between the model 5b and the standard at $z_{\text{reion}} \simeq 6$ and the dash-dot line $D_{5c,s}$ between 5c and the standard at $z_{\text{reion}} \simeq 6$. The thick-dotted ($f_{\text{sky}} = 0.65$) and solid lines ($f_{\text{sky}} = 1$) represent the cosmic variance limit for the *Planck* missions.

Cen R., ApJ submitted (astro-ph/0210473)

de Bernardis P. et al., 2000, Nat, 404, 955

Doroshkevich A. G., Naselsky I. P., Naselsky P. D., Novikov I. D., 2003, ApJ in press

Doroshkevich A. G., Naselsky P. D., 2002, Phys. Rev. D, 65, 13517

Fixen D. J., Cheng, E. S., Gales, J. M., Mather J. C., Shafer R. A., Wright E. L., 1996, ApJ, 473, 576

Kogut A. et al., 2003, ApJ submitted (astro-ph/0302213)

Halverson N. W. et al., 2002, ApJ, 568, 38

Hanany S. et al., 2000, ApJ, 545, L5

Hinshaw G. et al., 2003, ApJ submitted (astro-ph/0302217)

Ivanov P. B., Naselsky P. D., and Novikov I. D., 1994, Phys. Rev. D, 50, 71731

Jones B. J. T., Wyse R., 1985, A&A, 149, 144

Kotok E. V., Naselsky P. D., 1998, Phys. Rev. D, 58, 3517

Kovac J. et al., 2002, nat, 420, 772

Leitch E. M. et al., 2002, nat, 420, 763

Mandolesi, N. et al., 1998, *Planck* Low Frequency Instrument, A Proposal Submitted to ESA

- Mason B. S. et al., ApJ submitted (astro-ph/0205384)
Naselsky P. D., Novikov I. D., 2002, MNRAS, 334, 137
Naselsky P. D., 1978, Pis'ma v Astron. J. (Russian), 4, 387
Peebles P. J. E., 1968, ApJ, 153, 1
Peebles P. J. E., Seager S., Hu W., 2000, ApJ, 539, L1
Puget, J. L. et al., 1998, High Frequency Instrument for the
Planck Mission, A Proposal Submitted to ESA
Seager S., Sasselov D. D., Scott D., 2000, ApJS, 128, 407
Seljak U., Zaldarriaga M., 1996, ApJ, 469, 437
Verde L. et al., 2003, ApJ submitted (astro-ph/0302218)
Watson R. A. et al., MNRAS submitted (astro-ph/0205378)
Zabotin N. A., Naselsky P. D., 1982, Sov. Astron., 26, 272
Zel'dovich Ya. B., Kurt V., Sunyaev R. A., 1968, Zh. Eksp. Theor.
Phys., 55, 278